53rd AIAA/ASME/ASCE/AHS/ASC Structures, Structural Dynamics and Materials Conference
20th AI
23 - 26 April 2012, Honolulu, Hawaii

AIAA 2012-1763

A Statistics-Based Material Property Analysis to Support Ablation Simulation UQ Efforts

Sean R. Copeland*
Stanford University, Stanford, CA 94305, U.S.A.

Milad Mahzari †
Georgia Institute of Technology, Atlanta, GA 30332, U.S.A.

Ioana Cozmuta‡
STC Inc., NASA Ames Research Center, Moffett Field, CA 94035, U.S.A.

Juan J. Alonso§
Stanford University, Stanford, CA 94305, U.S.A.

Accurate characterization of Thermal Protection System (TPS) material properties is an important component in modeling and simulating the response of the material under heating. Unfortunately, for many common TPS materials, especially ablators, these material properties are not always well known and contribute a source of aleatory uncertainty to thermal simulations, impacting the safety and reliability of entry systems. Furthermore, efforts to capture these uncertainties have been hampered by a lack of suitable experimental data to establish proper input statistics, necessitating the use of ad-hoc methodologies to fabricate input PDFs. In this work, new ablator material property data from the Mars Science Laboratory (MSL) program is used to construct experimentally-based material property PDFs for use in non-deterministic ablation simulations. A standard UQ propagation, sensitivity analysis and uncertainty contributor breakdown analysis is performed using the revised input set in the anticipated MSL aerothermal environment. Lastly, a problem is formulated to quantitatively establish the relationship between errors in input statistics and errors in output quantities of interest.

Nomenclature

c_p	Specific heat
C_H	Convective heat transfer coefficient
h	Enthalpy
$\dot{m}$	Mass flow rate
q	Heat rate
$\dot{s}$	Surface recession rate
T	Temperature
u_e	Boundary layer edge velocity
x	Coordinate system moving with the recessing surface
y	Fixed coordinate system
α	Absorptivity
ϵ	Emissivity
Γ	Resin volume fraction

*Ph.D. Candidate, Department of Aeronautics & Astronautics, AIAA Student Member.
†Ph.D. Candidate, Daniel Guggenheim School of Aerospace Engineering, AIAA Student Member.
‡Senior Research Scientist, Aerothermodynamics Branch, Member AIAA.
§Associate Professor, Department of Aeronautics & Astronautics, AIAA Senior Member.

κ	Thermal conductivity
μ	Population mean
σ	Population standard deviation
ρ	Density
θ	Time

Acronyms

EDL	Entry, Descent and Landing
FIAT	Fully Implicit Ablation and Thermal Analysis Program
MEDLI	Mars Science Laboratory Entry Descent and Landing Instrumentation
MSL	Mars Science Laboratory
PDF	Probability Density Function
PICA	Phenolic Impregnated Carbon Ablator
QMU	Quantification of Margins and Uncertainties
QoI	Quantitiy of Interest
TC	Thermocouple
TPS	Thermal Protection System

Subscripts

A	Resin constituent A
B	Resin constituent B
C	Ablator reinforcing material C
c	Char
g	Pyrolysis gas
R	Radiation
v	Virgin
w	Wall or surface

I. Introduction

Objects traveling at hypersonic velocities through planetary atmospheres are subjected to extremely harsh environmental conditions. Strong shock waves generated by the passage of the object through the gas medium convert the kinetic energy present in the free stream to internal energy, resulting in high temperature, chemically reactive flow fields near the object. Surviving these environmental conditions requires the use of Thermal Protection Systems (TPS) to mitigate heat transfer to the vehicle's critical systems and substructure. This is accomplished by re-radiating energy at the surface back to the surrounding environment, and, in some cases, via thermal decomposition and ablation.

High-fidelity analysis and simulation capabilities have been developed over the past half-century to deliver analysis and design tools for sizing TPS systems and for performing safety and reliability assessments. Despite these efforts, significant errors and uncertainties persist that limit the accuracy, and consequently, the utility, of this predictive capability. The taxonomy of these uncertainties is as follows:

1. *Aleatory* - These uncertainties arise from natural variation in the model parameters or boundary conditions. For ablation simulations, these can be from a host of sources, including (but not limited to): finite manufacturing tolerances, material property non-uniformity, random atmospheric variation, etc.

2. *Epistemic* - These uncertainties and errors emerge from a lack of knowledge about the problem or the method by which the problem is solved. Examples of epistemic uncertainties include: improper input characterization, errors in the form of the governing equations, incomplete physical models, numerical errors from the discretization and solution of the governing equations, etc.

Historically, these errors and uncertainties have been mitigated by conservative design methods, expert judgement, experience and good engineering practice. However, more aggressive science and exploration missions (such as NASA's Mars Science Laboratory) are pushing missions into aerothermal environments where no experience, or experimental data exists, calling into question the reliability and safety of these new systems, and necessitating new design and analysis methodologies.

In recognition of this need, the Hypersonics branch of NASA's Fundamental Aeronautics Program has initiated a strategic plan[13] to identify sources of uncertainty as part of a comprehensive effort to develop new physics-based models for hypersonic systems, and to apply standard uncertainty quantification methodologies to existing high-fidelity analysis tools. Over the past decade, numerous analyses have been performed using a probabilistic interpretation of aleatory uncertainty to establish TPS reliability. Monte Carlo methodologies have been applied to uncertain parameters in ablation[6,9,17] and aerothermal[2,3] models, to determine the effect on imposed heating, subsurface temperatures, and surface recession levels. These approaches have given rise to new methods for assessing TPS margin[8] and have been the basis for new design and risk assessment methodologies.

However, gaps and limitations exist in the current body of work, particularly related to the characterization of the input probability density functions used to represent uncertain parameters. This is due in large part to a lack of large experimental datasets to accurately characterize input statistics and the relationships between inputs. As a consequence, input distributions for the cited analyses have been generated using largely ad-hoc approaches, with assumptions of PDF functional form, statistical moments, and parameter independence. Furthermore, there has been little emphasis placed on determining the effect these assumptions have on output statistics and reliability metrics.

This work addresses the highlighted issues with the following primary research goals:

1. *Construct an* experimentally-based *set of probability density functions for ablator material properties.*
2. *Perform a standard uncertainty propagation, contributor breakdown, and sensitivity analysis for a problem of relevance to the ablation modeling community.*
3. *Characterize the errors output PDFs as functions of the quality of the input distributions.*

This approach enables intelligent design of experiments to efficiently capture the most important contributors to overall uncertainty; attempts to quantitatively establish the relationship between input quality and output error; establishes the expected spread to quantities of interest, highlighting potential sources of epistemic uncertainty in the model as flight data becomes available; and constructs a seamless process by which experimental test results are incorporated directly into the analysis. Governing equations and physical models are outlined in Section II. The details of the analysis procedures described above are in Section III and results of the three step approach can be found in Section IV.

II. Model

Results presented in this work are generated using the Fully Implicit Ablation and Thermal Analysis Program (FIAT),[5] developed at NASA's Ames Research Center. This software package represents the state-of-the-art and has been used in the analysis and design processes for many flagship NASA missions, including, Galileo, Stardust, and MSL.

FIAT solves a system of four coupled partial differential equations to determine heat transfer through the TPS material. These four governing equations are supplemented with additional auxiliary equations modeling specific source terms, that will not be discussed in this work. For a full listing, refer to the original source material.[5]

A. Internal Energy Balance Equation

The internal energy balance equation is a transient thermal conduction problem with radiation and pyrolysis contributions:

$$\rho c_p \left.\frac{\partial T}{\partial \theta}\right|_x = \frac{\partial}{\partial x}\left(\kappa \frac{\partial T}{\partial x} - q_R\right)_\theta + \left(h_g - \bar{h}\right)\left.\frac{\partial \rho}{\partial \theta}\right|_y + \dot{s}\rho c_p \left.\frac{\partial T}{\partial x}\right|_\theta + \dot{m}_g \left.\frac{\partial h_g}{\partial x}\right|_\theta . \tag{1}$$

As the ablator material pyrolyzes, chars, and subsequently ablates, the surface of the material recedes. The x coordinate moves with this ablation front, while the y axis remains fixed. The terms in Eq. (1) can be interpreted as: the accumulation of sensible energy, net rate of conduction and radiative heat fluxes, rate of energy consumed during the pyrolysis process, convection rate of sensible energy due to a moving coordinate system, and the rate of energy convection from pyrolysis gas.

B. Internal Decomposition Equation

The ablator material is modeled as a three component composite material, where two materials A and B for the resin filler are mixed with a reinforcing material C in a volume fraction dictated by the input parameter Γ:

$$\rho = \Gamma\left(\rho_A + \rho_B\right) + \left(1 - \Gamma\right)\rho_C. \tag{2}$$

Each component decomposes independently according to a model based on an activation temperature for each constituent.

C. Internal Mass Balance Equation

As ablator material thermally decomposes, its density changes from that of the virgin material to a less-dense charred state, producing pyrolysis gasses that are ejected from the material into the surrounding flowfield. The continuity equation captures this mass transfer by assuming quasi-1D flow and an impermeable substructure:

$$\frac{\partial \dot{m}_g}{\partial y} = \frac{\partial \rho}{\partial \theta}. \tag{3}$$

D. Surface Energy Balance Equation

The surface energy balance dictates the heating to the TPS material due to the imposed aerothermal environment, capturing convective, radiative, and surface thermochemical effects between the ablator and the surrounding flowfield:

$$\rho_e u_e C_H\left(H_r - h_w\right) + \dot{m}_c h_c + \dot{m}_g h_g + \alpha q_{rad} = \left(\dot{m}_c + \dot{m}_g\right) h_w + \sigma \epsilon_w T_w^4 + q_{cond}. \tag{4}$$

Left hand side terms represent the contributions to the surface energy rate while the right hand side terms reject heat from the surface. Contributors the the surface energy include the sensible convective heat flux, the contribution to surface heat flux due to the moving coordinate system, the energy from the escaping pyrolysis gas, and the incoming radiative heat flux. Rejection of energy from the surface is due to energy released from the ablation process, energy re-radiated to the surrounding flowfield, and conduction into the the heatshield material. The convective heat transfer coefficient C_H employs a correction to account for the blowing of pyrolysis gasses at the surface.

III. Methodology

The analysis presented in this work addresses aleatory and epistemic sources of uncertainty pertaining to material properties for ablation simulations. The research objectives discussed in Section I will be approached in the following manner:

1. Construct *experiment-based* material property input PDFs to be used for non-deterministic ablation simulations. Determine the PDF functional form and establish dependencies between input parameters shown in the experimental data.

2. Propagate the established uncertainties through the material response model using a Monte Carlo methodology. Supplement the propagation with a finite-difference based sensitivity analysis and uncertainty contributor breakdown using Pearson's moment correlation coefficients and Sobol' global sensitivity indices.

3. Characterize errors in output quantities of interest (QoI's) as a function of input distribution quality on the basis of Kullback-Leibler divergence for several assumed input PDF functional types.

Details for each portion of the analysis will be supplied in Sections III.B, III.C, & III.D.

A. Problem Definition

NASA's most recent flagship mission, the Mars Science Laboratory, provides a unique opportunity for the ablation modeling community. A suite of instrumented plugs is embedded in the heat shield that will collect in-depth temperature measurements and the progression of an isotherm during the Entry, Descent and Landing (EDL) phase of the mission, currently scheduled for August 2012. This instrumentation will provide the largest volume of data ever collected in the Martian atmosphere to be used to infer the heating environment, to evaluate the performance of the thermal protection system, and to verify & validate high fidelity analysis tools. The MSL Entry, Descent and Landing Instrumentation (MEDLI) program is ideally suited to methodology proposed in this work and will be the focus of the analysis, but it should be emphasized that the approach presented is widely applicable to other problems of interest.

Parameter	
Virgin Density	ρ_v
Virgin Specific Heat	c_{p_v}
Virgin Thermal Conductivity	κ_v
Char Density	ρ_c
Char Specific Heat	c_{p_c}
Char Thermal Conductivity	κ_c

Table 1. PICA material model parameters carrying uncertainties.

A more detailed description of the anticipated aerothermal environments, the strategic placement of the instrumentation on the capsule forebody and a schematic of an instrumented plug is shown in Fig. (1). The placement of the sensor plugs is intended to inform scientists and engineers of the physical phenomena that are anticipated during the entry phase, including turbulent transition, and windside heating augmentation. Each sensor plug, denoted by the white dots in Fig. (1b), contains four embedded thermocouples and an isotherm detector. In total, the instrumentation will provide the time history of the temperature at four fixed depths and the progression of an isotherm through the material under the local heating conditions, shown in Fig. (1a). Location four of Fig. (1b) is the focus of the analysis presented here and was selected because of the benign anticipated heating conditions.

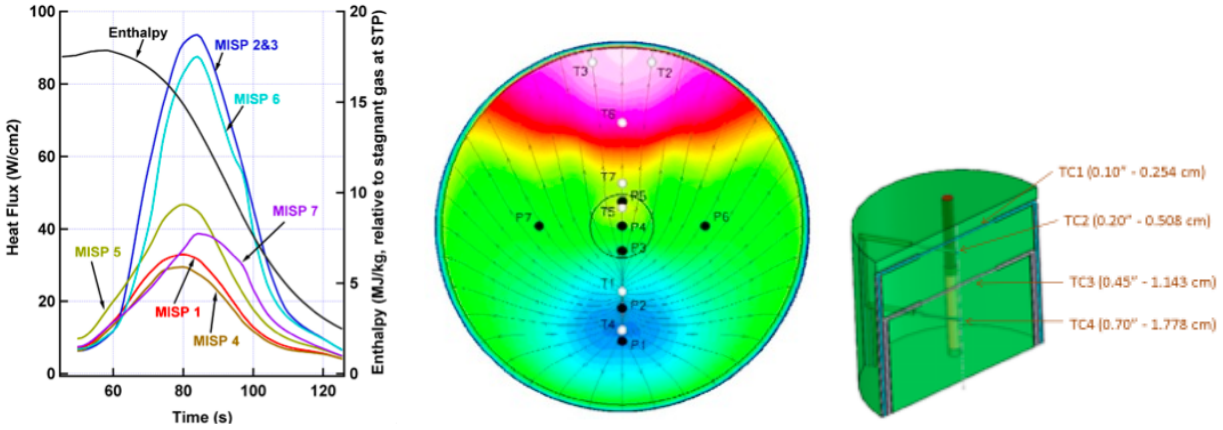

(a) Thermal environments. (b) Instrumentation layout. (c) MISP plug.

Figure 1. Mars Science Laboratory anticipated thermal environments, and embedded heat shield instrumentation.

As errors and uncertainties associated with the aerothermal environment and surface conditions are beyond the scope of this work, a special analysis strategy was developed. The anticipated surface conditions (characterized by time histories for wall recovery enthalpies, radiative flux, pressures, etc.) are used to generate nominal temperature profiles in the material. The time history of temperature at the thermocouple closest to the surface then becomes a boundary condition for a second simulation, permitting the elimination of the surface energy balance, Eq. (4), from the governing equation set and facilitates the examination of the ablation and thermal conduction problem for the remaining thermocouples. The schematic in Fig. (A) shows the procedure graphically.

B. Input Distributions

A set of revised input distributions for material properties is desired for use in future stochastic ablation simulations. An analysis of the available experimental data permits a determination of the functional form (if

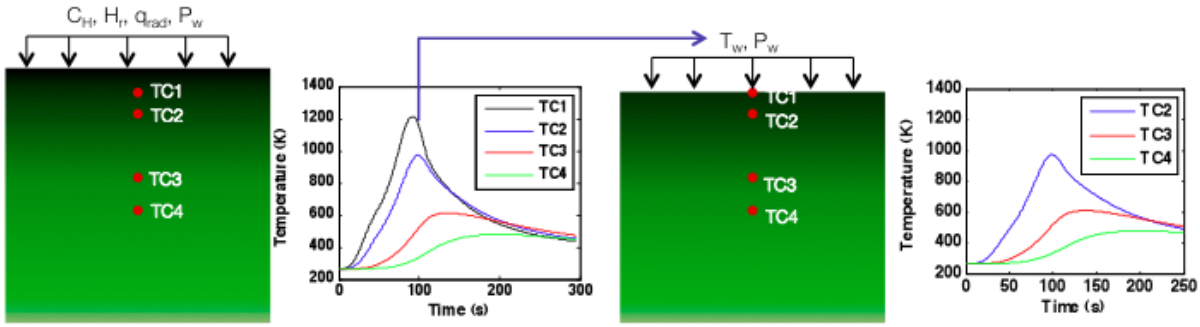

Figure 2. Time-dependent temperature and pressure boundary conditions for UQ propagation.

any) that best describes the trends seen in the data, and establishes relationships between material properties. This eliminates, to the greatest extent possible, the ad-hoc methodologies currently in use. Experimental data from the MSL TPS qualification effort is used for the analysis and is sufficient to establish statistics for a subset of the quantities of interest listed in Tab. (1). Further experimental testing, performed in support of the MEDLI program, will target the remaining parameters of interest, but is not currently available.

To determine the PDF functional form, the following approach is used. Means, standard deviations, covariances, and correlation coefficients are calculated for supported material properties (ρ_v, ρ_c, and κ_v) then used as parameters for candidate density functions. The experimental data is binned, and plotted as a histogram and compared the candidate functions based on the statistical parameters calculated from the data.

For the remaining parameters of interest where there is insufficient data to perform a statistical analysis (κ_c, Cp_v, Cp_v), alternative approaches are used. The functional form of the char thermal conductivity is assumed to be the same as what is used for its virgin counterpart. The mean value for the distribution is matched to the available data, and a standard deviation of 15% of its mean value is assumed. Covariance between virgin and char thermal conductivities is assumed to be equal to the covariance between virgin and char density. Specific heats are calculated via thermal diffusivity, α, shown in Eq. (5). A uniform distribution is assumed for thermal diffusivity, with mean values matching those from experiments and standard deviations of 5% of the means. Specific heat is then calculated via algebraic manipulation, incorporating previously sampled values of thermal conductivity and density.

$$\alpha = \frac{\kappa}{\rho c_p} \tag{5}$$

C. Uncertainty Analysis

The uncertainty propagation, contributor breakdown and sensitivity analysis utilizes the revised inputs and applies the observed uncertainties to a problem of relevance to the ablation modeling community, explained in detail in Section III.A. Each portion of the analysis targets information vital to understanding the behavior, expected variation, and sources of uncertainty within the model, that are both temporally and spatially dependent. As flight data becomes available, this detailed analysis forms the backbone of establishing ground-to-flight traceability between ground testing and simulation of the flight environment, and provides evidence that can be used to reconcile potential differences between the observed data and predictions.

1. Uncertainty Propagation

The propagation of uncertainties through the material response model is performed via a standard Monte Carlo method. Samples are drawn from the material property density functions constructed in III.B and used as inputs for the material response model. This process is repeated many times to collect statistics for the in-depth temperature at each of the thermocouple locations. Plotting these statistics provides a time evolution of the expected temperatures from the flight data and a region of confidence where in-depth temperatures are expected due to aleatory variations in material properties.

2. Sensitivity Analysis

The sensitivity analysis is performed using a standard finite-difference based approach to calculate gradients in temperature at each of the thermocouple locations with respect to the uncertain parameters. Nominal material property values are selected to be the mean values for each of the material properties. These nominal values are perturbed by 0.5% of their nominal value and the local gradient is calculated using central differencing about the nominal. These gradients give a pure measure how the model responds to perturbations to the input parameters and provide clues to the dominant physical processes being modeled at any given time and location.

3. Uncertainty Contributor Breakdown

The contributor breakdown is performed using two methods, Pearson's moment correlation coefficients and Sobol' global sensitivity indices. The correlation coefficient approach is prevalent in the existing ablation UQ literature and measures the strength of the linear dependence between the inputs and output QoI's. As the governing equations are inherently non-linear, it is not clear that this linear analysis accurately captures and ranks the primary uncertainty contributors. As an independent check, the results from the correlation coefficient analysis are checked with the results from the Sobol' method, which is capable of identifying non-linear relationships between inputs and outputs. By comparing the results, the adequacy of the correlation approach as it applies to ablation simulations can be evaluated.

D. Error Analysis

The results of the error analysis are aimed toward quantitatively assessing how the quality of the input distributions affects the statistics of output quantities of interest. In particular, it addresses the question of, "how much investment is required to adequately resolve my safety and reliability metrics?" To accomplish this, a problem is fabricated in the following manner:

1. Assume there exists some 'true' distribution(s) representing aleatory uncertainties for material properties.
2. From that true distribution, we draw a small number, N, samples, replicating the material testing process.
3. Using the data collected from the 'testing' phase, construct approximate probability density functions to be used in a UQ analysis. Approximate density functions are to be constructed under three assumptions:
   (a) The approximate input has the same functional form as the 'true' distribution.
   (b) The approximate inputs are independent gaussian random variables.
   (c) The approximate inputs are independent uniform random variables.
4. Perform a Monte Carlo analysis using $M >> N$ samples to achieve converged statistics for each assumed input type and for the 'true' inputs.
5. Calculate the error between the converged statistics using the approximate inputs and the converged statistics from the 'true' distribution.

By varying the number of samples drawn, N, and by evaluating the error from the input functional type, we can examine how the error is affected by additional investment in input characterization (experimental testing) and how the assumptions made during the formation of the inputs affects the accuracy of the results.

IV. Results

A. Input Probability Density Function

An examination of the MSL TPS qualification data for virgin density, char density, and virgin thermal conductivity supports the use of a multivariate normal distribution to represent ablator material properties

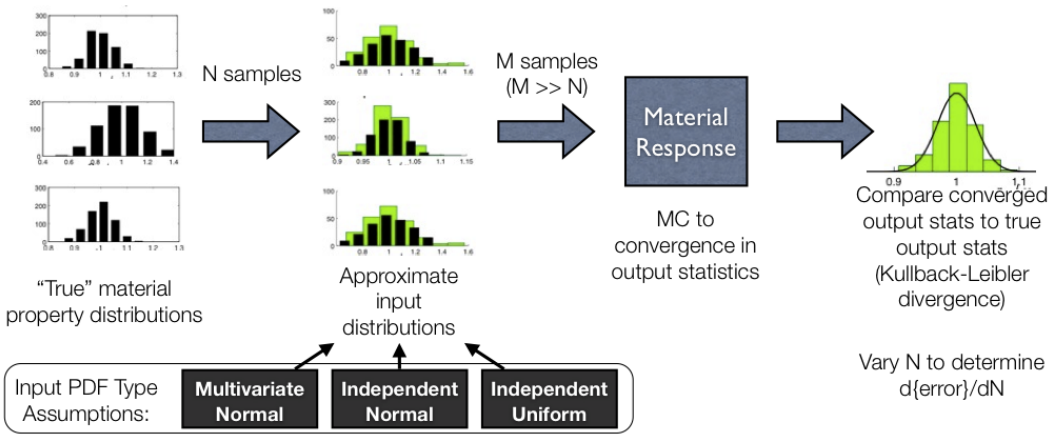

Figure 3. Block diagram showing the error analysis methodology.

(with special accommodation for unsupported parameters, described in Section III.B). Histograms of the data are co-plotted with marginal distributions with matching statistical parameters in Fig. (4a), showing good agreement between the experimental data and the presumed distribution. Fig. (4b) shows the dependencies observed between virgin and char densities, and between virgin density and thermal conductivity in scatter. Experimental data points are plotted in green, while samples drawn from the presumed distribution are plotted in black. Correlation coefficients and corresponding p-values are shown in Tab. (2) and Tab. (3) indicating statistical evidence to support dependence between the parameters. The importance of capturing these dependencies is highlighted in IV.E

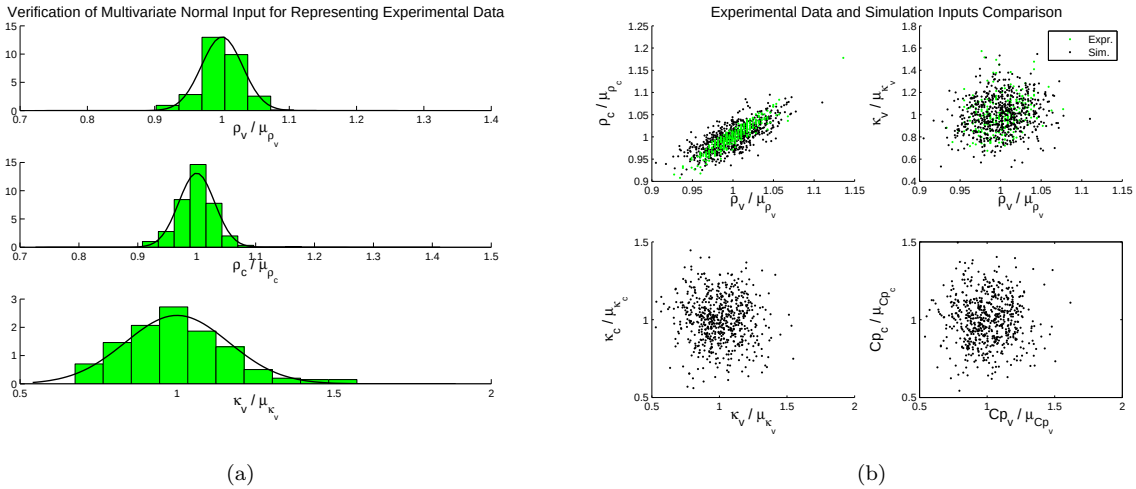

(a) (b)

Figure 4. Input PDF verification and validation

ρ_{ρ_v,ρ_c}	0.934
ρ_{ρ_v,κ_v}	0.242

Table 2. Correlation coefficients calculated from experimental data.

Fig. (5) plots samples from the presumed distribution for all parameters of interest, normalized by population mean. Where applicable, binned experimental data is co-plotted in green. An examination of the histograms and scatterplots shows the revised input distribution, based on a multivariate normal distribution that incorporates inter-parameter dependencies, accurately represents the available experimental data. As

p_{ρ_v,ρ_c}	0.000
p_{ρ_v,κ_v}	$2.86 * 10^{-4}$

Table 3. P-values coefficients calculated from experimental data.

additional experimental results become available, this assertion must be tested, particularly for char material properties.

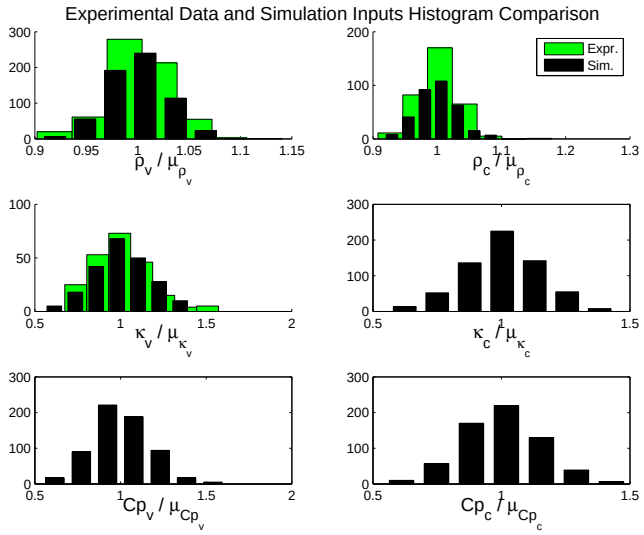

Figure 5. A comparison between experimental data and samples drawn from the constructed PDF

B. Uncertainty Analysis

A Monte Carlo methodology, using 2000 samples from the input density function from Section IV.A is used to propagate uncertainties through the material response model using the temperature-based boundary conditions described previously. Results from the stochastic analysis is shown in Fig. (7) for thermocouples 2, 3, and 4. Mean values are shown as solid lines, and three standard deviations from the mean are plotted as dotted lines, showing a band of expected temperature variation from the established material property uncertainties.

An alternate visualization of the data showing the evolution in the standard deviation of temperature in time for the thermocouples accompanies the envelope plot. Uncertainty to in-depth temperature is maximized at the peak heating conditions and decreases during the cool-down process, showing peak standard deviations of roughly 2.5% the mean value. This propagation analysis shows a reasonably narrow temperature band of anticipated temperature readings. This is advantageous for identifying potential sources of epistemic (model-form) uncertainties as

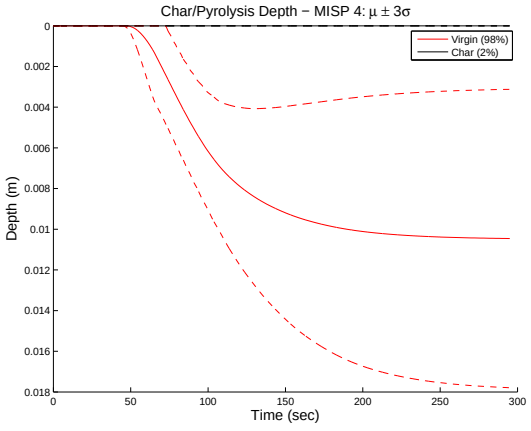

Figure 6. Expected virgin and char front depths.

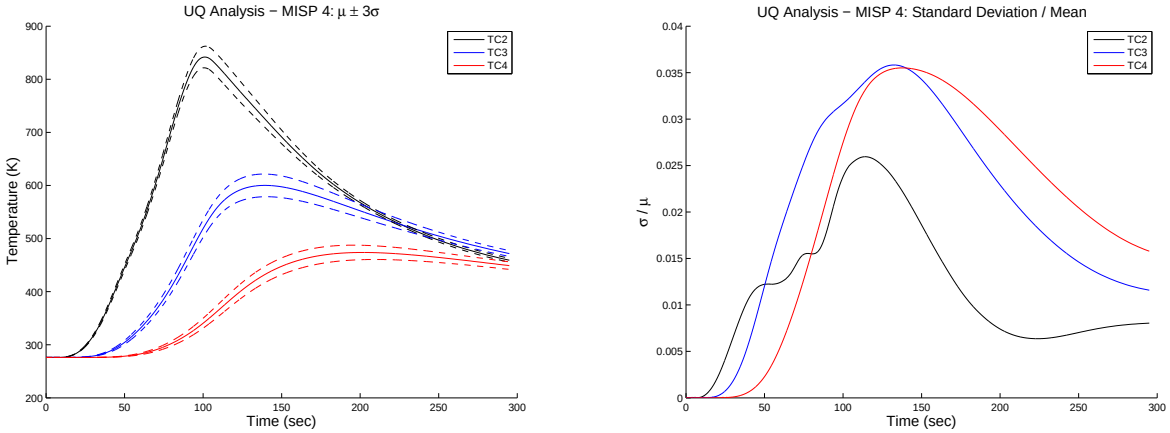

(a) (b)

Figure 7. MISP 4 propagation of uncertainties.

flight data becomes available.

The pyrolysis region is shown in Fig. (6) with mean and 3 standard deviations for the front position as it evolves in time. The 98% virgin line shows a large region where the onset of the pyrolysis zone begins. Under the applied heating conditions, the char region never fully forms and grows, shown by the char depth of zero in the figure. Simulation conditions indicate the possibility of a very wide pyrolysis zone (as much as two centimeters), indicating the need for good models during the material transition phase.

C. Finite-Difference Sensitivity Analysis

A central-difference approach using step sizes of 0.5% of the nominal material property values is used to calculate the gradient in temperature at each thermocouple depth. The stacked-area plots of Fig. (8) show the contribution of each of the vector components of the gradient (e.g. the areas of each of the colors at a vertical slice gives the relative contribution of that component to the norm of the gradient at that time). These gradient plots give a raw measure of the dominant effects present in the model under the time-dependent heating conditions at the three depths. Early, under benign heating, the sensitivity is split evenly between the virgin density, thermal conductivity, and specific heat, but as char formation begins to occur, the char density becomes a key parameter. As anticipated, thermocouple 2 shows the largest sensitivity to char properties, especially thermal conductivity, with these char parameters becoming less important deeper in the material.

D. Uncertainty Contributor Breakdown

The contributor breakdown is performed using both the common Pearson's correlation coefficient approach and the Sobol' index method and is shown in Fig. (9). Total uncertainty is normalized for both sets of plots at each time step, and is plotted using stacked areas (vertical slices of the plot give the relative contributions to overall uncertainty for a given point in time at a certain thermocouple depth). These contributor breakdowns differ from the pure sensitivity analysis, shown in the previous section, in that the variation of the parameter due to its input PDF is factored into the analysis. So, for the variation seen in Fig. (7) the corresponding vertical slice from the contributor breakdown shows which parameters are most responsible for the observed QoI variation.

It is interesting to note that discrepancies between the results of the correlation and Sobol' approaches exist. These discrepancies are highlighted in Fig. (10), Fig. (11), and Fig. (12). Correlation and Sobol' results for each parameter are co-plotted, highlighting differences in the evolution of their overall contribution to uncertainty. To make the effects of these discrepancies more apparent, the time-dependent ranks of each uncertainty contributor are plotted using the two methods, showing how the discrepancies in contributor evolution affect the overall ranking of primary uncertainty contributors. These dissimilarities between the

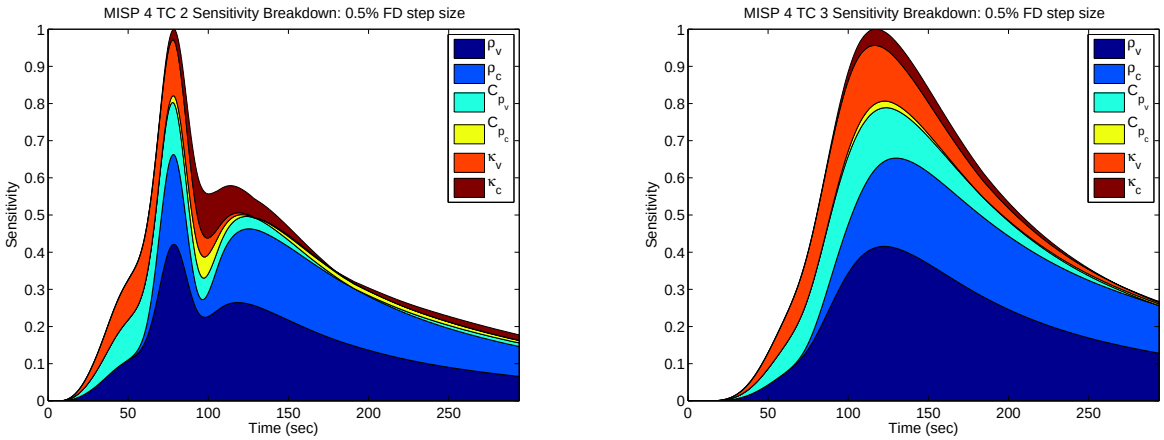

(a) TC 2

(b) TC 3

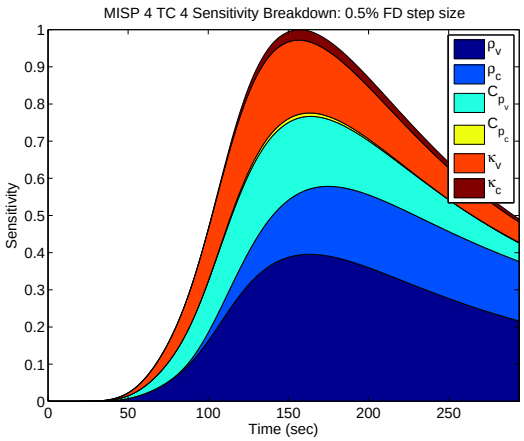

(c) TC 4

Figure 8. MISP 4 finite-difference sensitivity analysis.

methods highlights the dangers of using linear methods to draw conclusions on inherently non-linear systems, and makes a strong case for the use of Sobol' indices for future contributor breakdown studies.

E. Error Analysis

The error analysis strategy detailed in Section III.D is performed using the maximum TC4 temperature as the quantity of interest. This particular quantity is used as a surrogate for the bond line temperature (the temperature at the base of the TPS where the heat shield and vehicle substructure are bonded together), which is a common design criteria for TPS sizing. The 'true' distribution is defined as the input density function from IV.A. Converged statistics between the truth and approximate inputs are compared for the three assumed input PDF functional forms ('truth', independent normal, and independent uniform random variables) and are shown in Fig. (13). Qualitatively, the assumption of independent variables reduces the variance in the QoI. Variation in the output QoI is aggravated by positive correlation between the virgin and char materials that is not accurately captured if the parameter dependence is not established. For example, a higher virgin thermal conductivity implies a higher char thermal conductivity, hence a much larger difference in temperature than if this dependence were not captured.

A calculation of the Kullback-Liebler divergence between the truth and approximate distributions is shown in Fig. (14). The error shows insensitivity to the number of sample draws, N, as expected from the Monte Carlo based approach upon which the approximate distributions are formed, but does show significant sensitivity to input PDF functional type assumptions. Error dramatically increases as the input PDF type

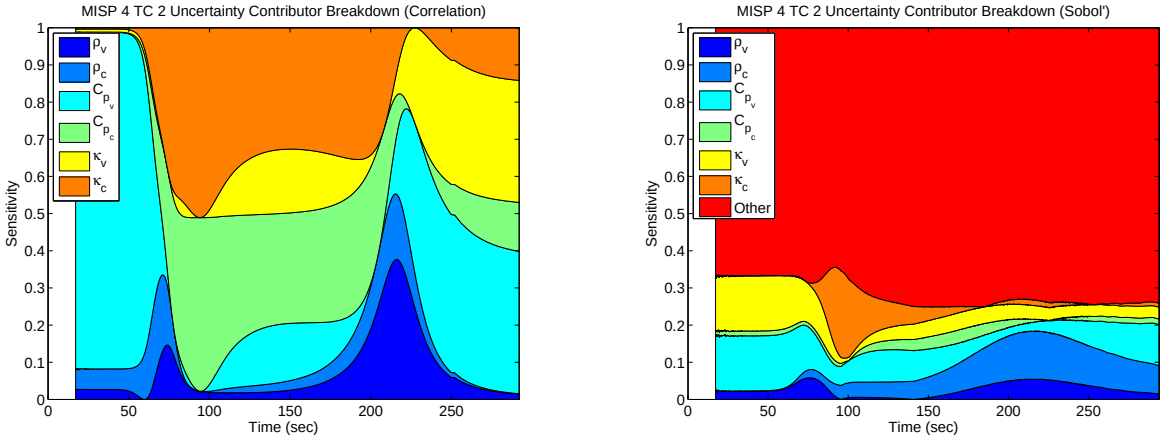

(a)

(b)

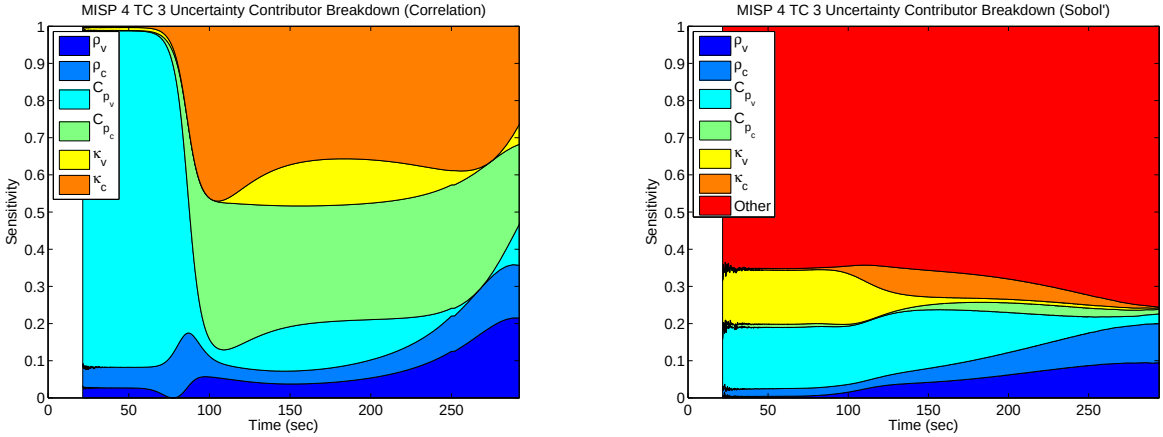

(c)

(d)

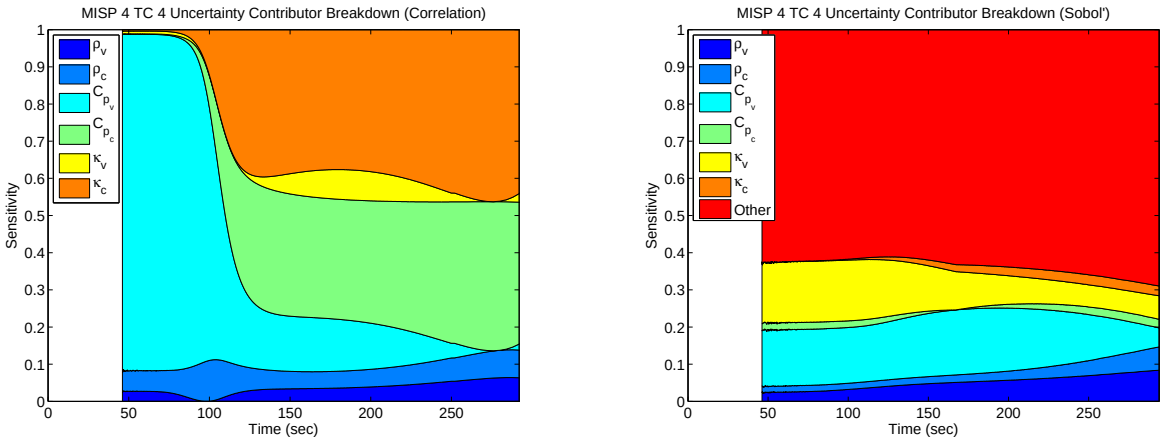

(e)

(f)

Figure 9. Comparison of correlation coefficient and Sobol' index contributor breakdowns for plug 4.

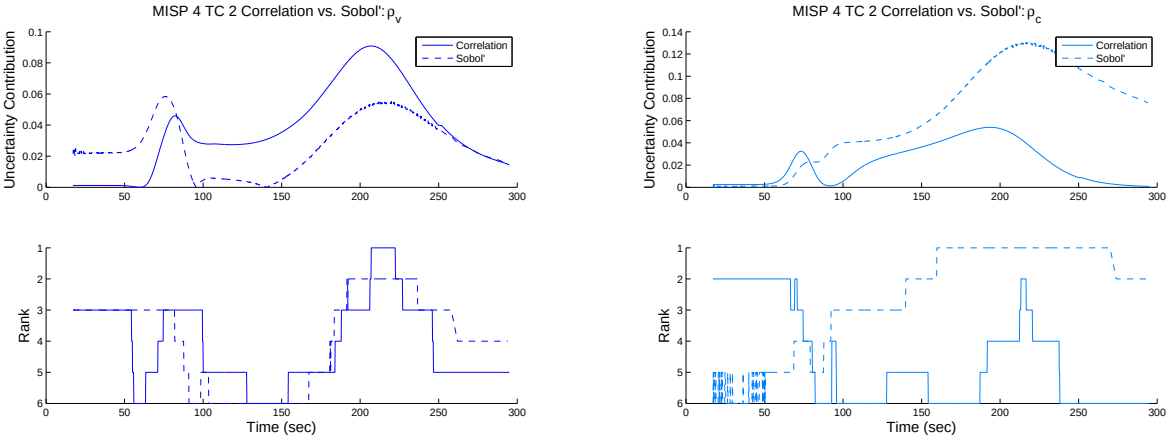

(a)

(b)

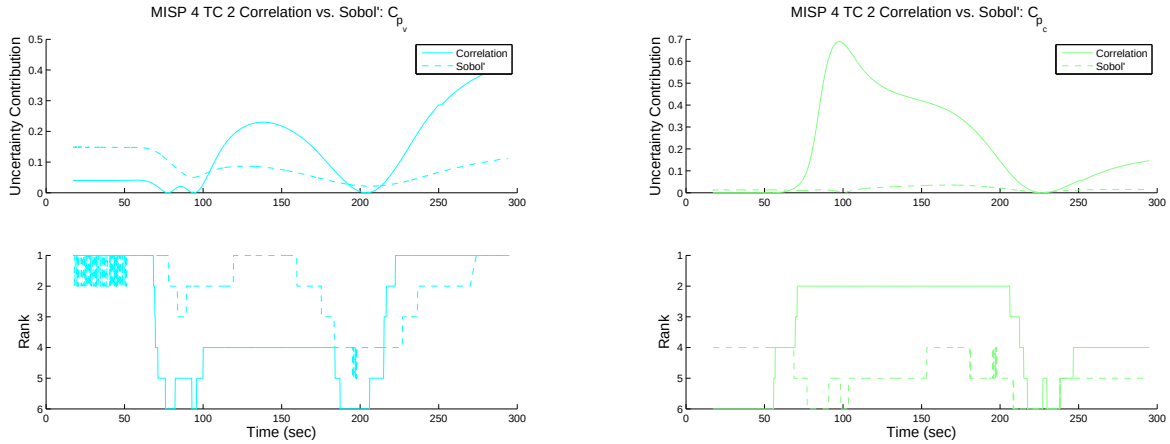

(c)

(d)

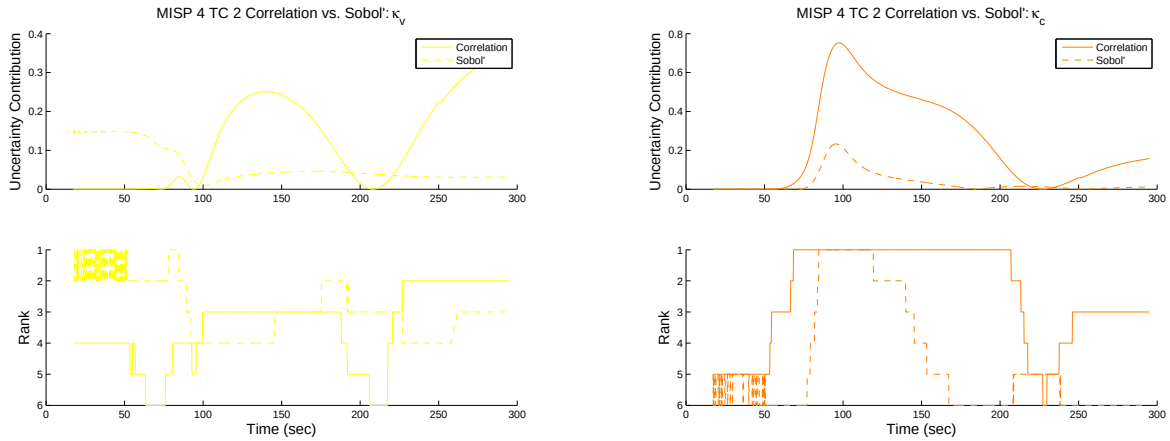

(e)

(f)

Figure 10. Comparison of Sobol' and correlation coefficients at TC 2.

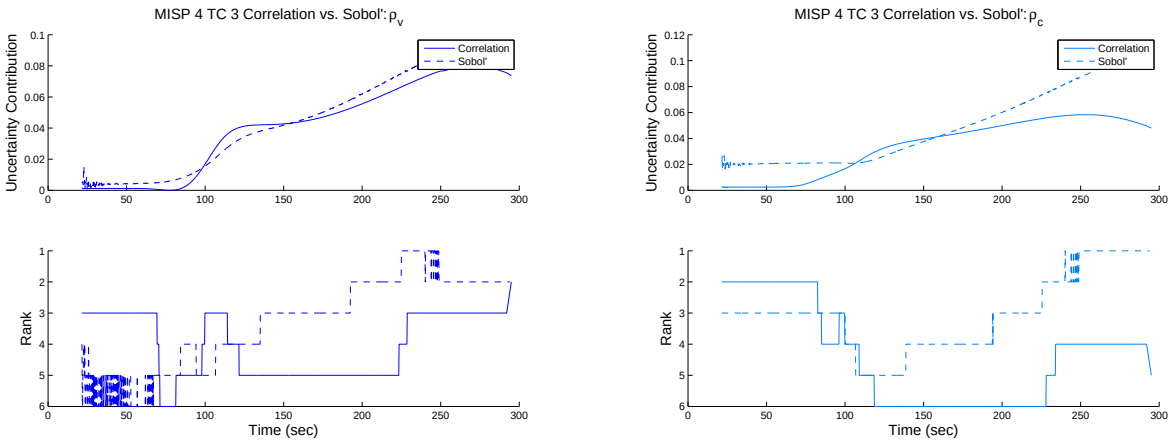

(a)

(b)

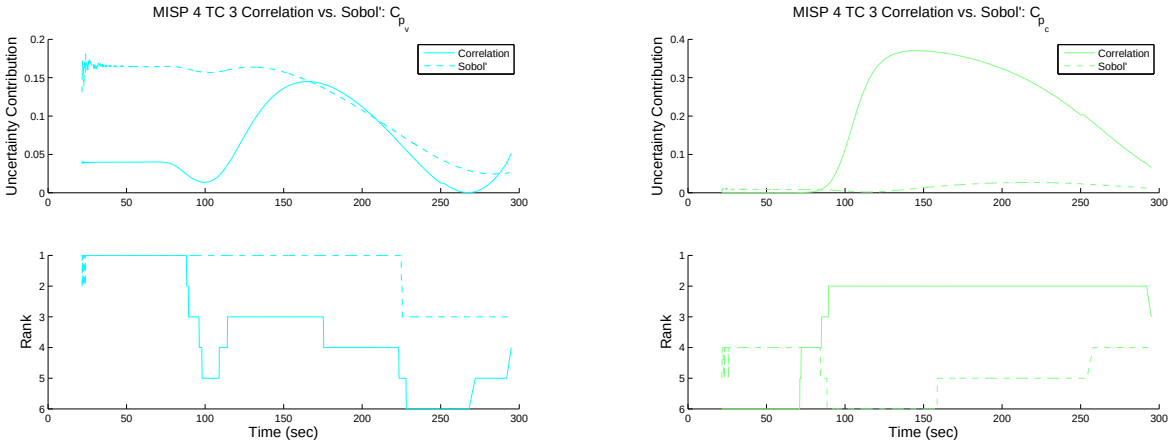

(c)

(d)

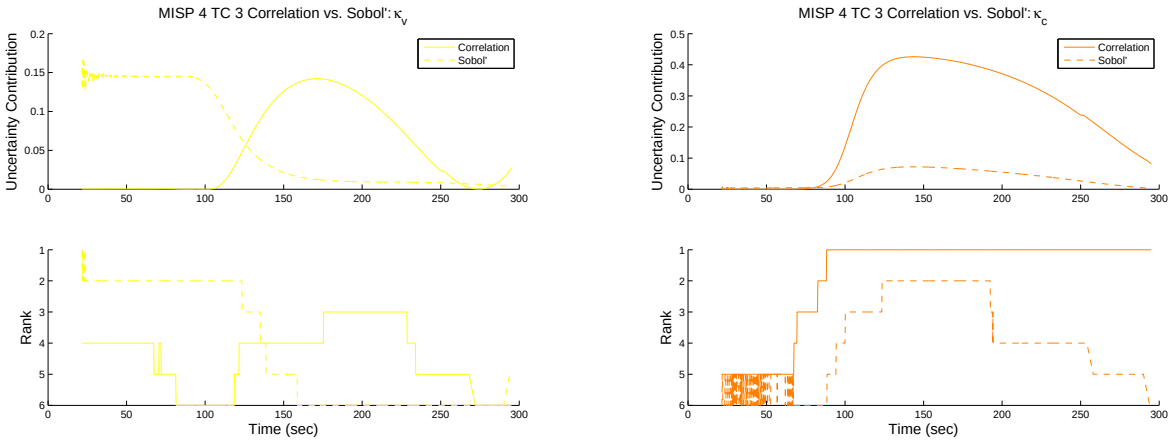

(e)

(f)

Figure 11. Comparison of Sobol' and Correlation Coefficients at TC 3.

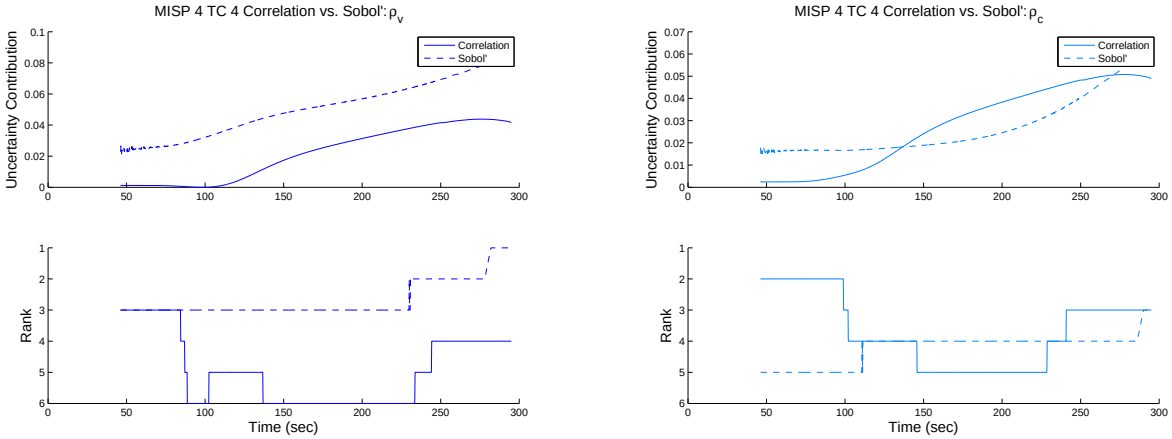

(a)

(b)

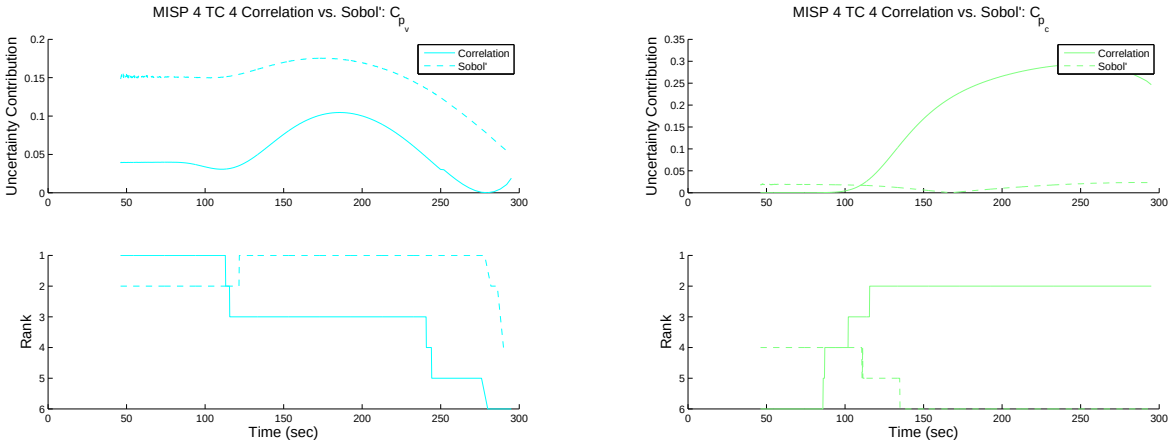

(c)

(d)

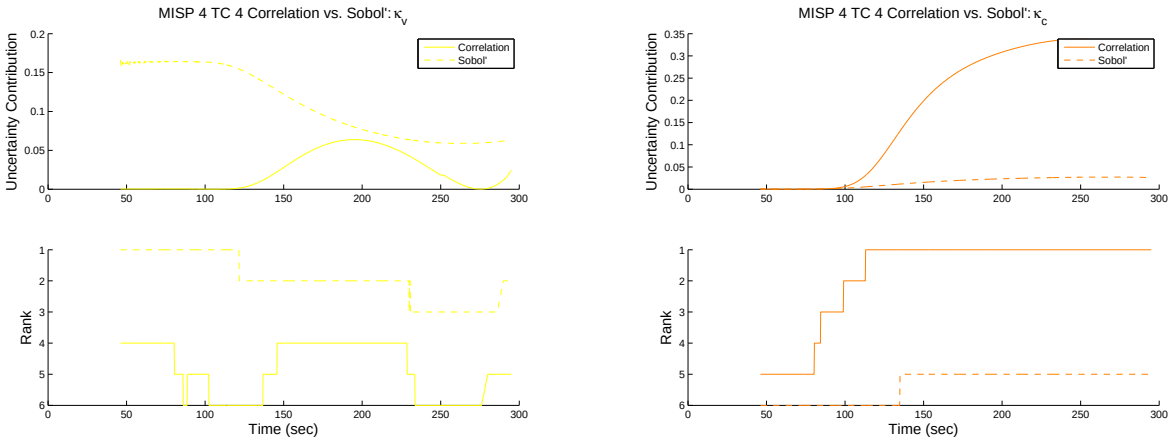

(e)

(f)

Figure 12. Comparison of Sobol' and Correlation Coefficients at TC 4.

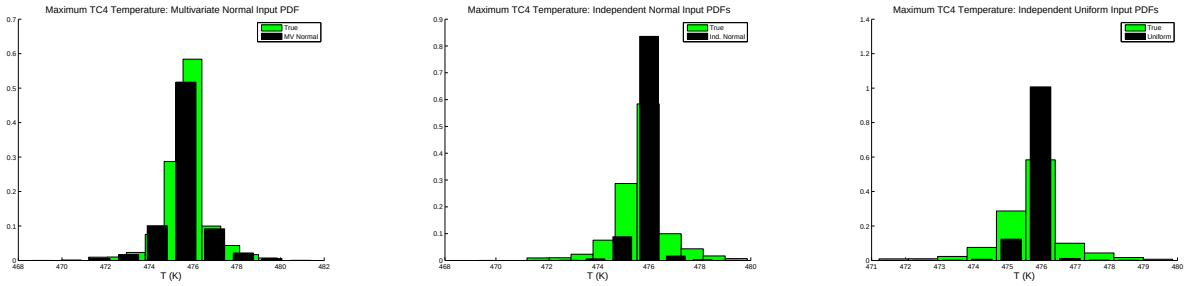

(a) Multivariate normal (b) Independent normal (c) Independent uniform

Figure 13. Comparison of converged output statistics from the 'true' distributions and the approximate input distributions.

diverges further from the truth distribution, and parameter dependence assumptions are relaxed.

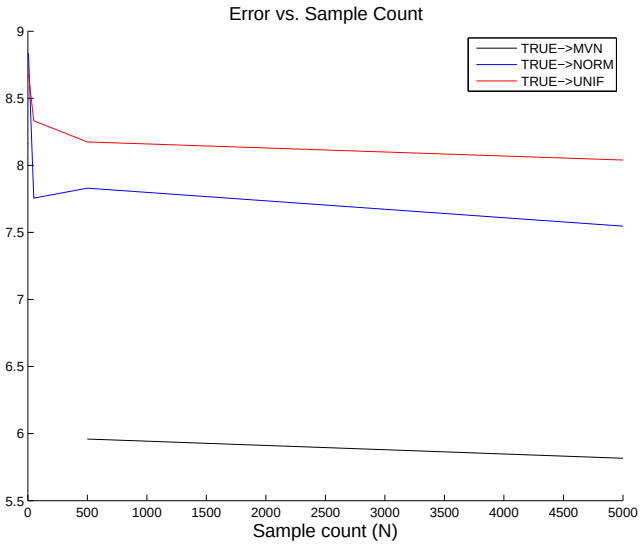

Figure 14. The effect of sample count, N, and independence assumptions on output error.

This analysis shows the importance of properly replicating observed data with appropriate PDF types. Furthermore, it emphasizes the importance of characterizing the relationships between material property parameters, as independence assumptions contribute significantly to the overall error in the output statistics, potentially impacting design metrics in a non-conservative fashion.

V. Conclusions

A comprehensive material property analysis was performed using available data from the MSL TPS qualification effort, in conjunction with state-of-the-art high-fidelity material response modeling tools to assess the affects of material property characterization on UQ efforts for ablation simulations. The following conclusions and assertions can be made from the results shown in Section IV:

1. The available material property data for virgin density, char density, and virgin thermal conductivity supports the use of a multivariate normal distribution to faithfully represent observed trends. Furthermore, there is statistically significant evidence to support that the material property parameters are dependent on one another and that it is important to capture those dependencies when performing UQ analyses, necessitating the development of a unified material model or a greater investment in material

property testing.

2. The expected variation to in-depth temperature due to aleatory material property uncertainties is relatively small, facilitating efforts to reconstruct surface environmental conditions and to establish or refute sources of epistemic (model-form) uncertainties in existing state-of-the-art material response codes. Correlation coefficient and Sobol' global sensitivity indices show discrepancies in the primary uncertainty contributors, emphasizing the need to capture outputs from the non-linear governing equations using non-linear approaches to prevent false accounting.

3. Output QoI error shows insensitivity to high volumes of material property testing, but shows great sensitivity to assumed input forms (as expected based on the Monte Carlo approach used). This emphasizes the need to perform sufficient testing to establish the functional forms and inter-parameter dependencies for simulation inputs, at a minimum.

Acknowledgments

The authors would like to thank the MEDLI program by which this research was funded. Sean R. Copeland would like to thank the Lillie family for their generous support of the Stanford Graduate Fellowship program. Additionally, the input and suggestions to this research from Karthik Duraisamy, Deepak Bose, and Paul George Constantine are greatly appreciated.

References

[1]Anderson, J. D., *Hypersonic and High-Temperature Gas Dynamics*, AIAA Education Series, Reston, 2006.

[2]Bose, D., Wright, M., Gökçen, T., "Uncertainty and Sensitivity Analysis of Thermochemical Modeling for Titan Atmospheric Entry," *AIAA 2004-2455*, 37^{th} AIAA Thermophysics Conference, Portland, OR, 2004.

[3]Bose, D., Wright, M., "Uncertainty Analysis of Laminar Aeroheating Predictions for Mars Entries," *AIAA 2005-4682*, 38^{th} AIAA Thermophysics Conference, Toronto, Ontario Canada, 2005.

[4]Chen, Y.-K., and Milos, F. S., Fully Implicit Ablation and Thermal Analysis Program (FIAT), *ICCE/4, Fourth International Conference on Composites Engineering*, edited by D. Hui, International Community for Composites Engineering and College of Engineering, Univ. of New Orleans, New Orleans, LA, 1997, pp. 661, 662.

[5]Chen, Y.-K., Milos, F.S., Ablation and Thermal Response Program for Spacecraft Heatshield Analysis, Journal of Spacecraft and Rockets, Vol. 36, No. 3, May-June 1999.

[6]Chen, Y.-K., Squire, T., Laub, B., Wright, M., "Monte Carlo Analysis for Spacecraft Thermal Protection System Design," *AIAA 2006-2951*, 9^{th} AIAA/ASME Joint Thermophysics and Heat Transfer Conference, San Francisco, CA, 2006.

[7]Users Manual: Aerotherm Charring Material Thermal Response and Ablation Program, Aerotherm Div., Acurex Corp., Mountain View, CA, Aug. 1987.

[8]Cozmuta, I., et. al, "Defining Ablative Thermal Protection System Margins for Planetary Entry Vehicles", *AIAA 2011-3757*, 42nd AIAA Thermophysics Conference, Honolulu, HI 2011.

[9]Dec, J. A., Mitcheltree, R. A., "Probabilistic Design of a Mars Sample Return Earth Entry Vehicle Thermal Protection System," *AIAA 2002-0910*, 40^{th} AIAA Aerospace Sciences Meeting & Exhibit, Reno, NV 2002.

[10]Edquist, K. T., Dyakonov, A. A., Wright, M. J., Tang, C. Y., "Aerothermodynamic Design of the Mars Science Laboratory Heatshield," *AIAA 2009-4075*, 41^{st} AIAA Thermophysics Conference, San Antonio, TX, 2009.

[11]Gazarik, M., Wright, M., Little, A., Cheatwood, F., Herath, J., Munk, M., Novak, J., and Martinez, E., Overview of the MEDLI Project, IEEE Aerospace Conference, Big Sky, MT, No. IEEEAC paper No. 1510, 2008.

[12]Laub, B., Chen, Y.-K., Dec, J. A., "Development of a High-Fidelity Thermal/Ablation Response Model for SLA-561V," *AIAA 2009-4232*, 41^{st} AIAA Thermophysics Conference, San Antonio, TX, 2009.

[13]Mansour, N., Pittman, J., Olson, L., "Fundamental Aeronautics Hypersonics Project: Overview," *AIAA 2007-4263*, 39^{th} AIAA Thermophysics Conference, Miami, FL, June, 2007.

[14]McGuire, M. K., Bowles, J. V., Yang L. H., Kinney, D. J., Roberts, C. D., "TPS Selection and Sizing Tool Implemented in an Advanced Engineering Environment," *AIAA 2004-342*, 42^{nd} AIAA Aerospace Sciences Meeting & Exhibit, Reno, NV 2004.

[15]Moyer, C. B., and Rindal, R. A., An Analysis of the Coupled Chemically Reacting Boundary Layer and Charring Ablator, Part II, Finite Difference Solution for the In-Depth Response of Charring Materials Considering Surface Chemical and Energy Balances, NASA CR-1061, June 1968.

[16]Rasmussen, C. E., and Williams C., *Gaussian Processes for Machine Learning*, MIT Press, Cambridge, 2006.

[17]Sepka, S. A., Wright, M., "Monte Carlo Approach to FIAT Uncertainties with Applications for Mars Science Laboratory," Journal of Thermophysics and Heat Transfer, Vol. 25, No. 4, October-December 2011.

[18]Stackpoole, M., Sepka, S., Cozmuta, I., Kontinos, D., "Post-Flight Evaluation of Stardust Sample Return Capsule Forebody Heatshield Material," *AIAA 2008-1202*, 46^{th} AIAA Aerospace Sciences Meeting & Exhibit, Reno, NV, 2008.

[19]White, T., et. al, "Proposed Analysis Process for Mars Science Laboratory Heat Shield Sensor Plug Flight Data", *AIAA 2011-3957*, 42nd AIAA Thermophysics Conference, Honolulu, HI 2011.

[20]Wright, M. J., et. al, "A Review of Aerothermal Modeling for Mars Entry Missions", *AIAA 2010-443*, 48th AIAA Aerospace Sciences Meeting Including the New Horizons Forum and Aerospace Exposition, Orlando, FL 2010.